An Examination of a Phase Domain Modeling of Untransposed Transmission Lines

Tomoatsu Ino
Electrical Engineering Dept.
Kanagawa University
Yokohama, 221-8686, Japan
tino@cc.kanagawa-u.ac.jp

Masahiro Sekita
Corporate Planning & Administration Dept.
Electric Power Development Co., Ltd.
Tokyo, 104-8165, Japan
den09375@epdc.co.jp

Junji Sawada
Electric Power System Dept.
Kaihatsu Computing Service Centre Ltd.
Tokyo, 113-8451, Japan
sawada@kcc.co.jp

Abstract - **This paper examines a phase domain modeling for lager time span of simulation. First, a successive approximation of frequency dependent using low order transfer function and a DC expression for lower frequency area are introduced. Next, the comparison between field tests and simulated results with the model are made for impulse energizing. Lastly, for comparatively larger time span of simulation, comparison between the model and a constant transformation matrix model results are made. From these results, this paper concluded phase domain model is the more important in the larger time span of simulation.**

Keywords: Transmission Line, Untransposed Line, Transient Analysis, Phase Domain Modeling

1. INTRODUCTION

Recently, It becomes clear that the detailed modeling in modal expression for untransposed transmission lines is limited mainly because of the difficulty of the physical causality realization in the single transformation matrix representation including surge admittance [1,7]. Several phase domain modelings have been developed [3-6, 8] , overcoming the weakness of modal expression. These papers verify their efficiency and accuracy for comparatively small time span of simulation. Then there is still room to examine long run behavior of the phase model with comparison to the constant matrix model. Also comparison work between field tests and the phase domain model is still few. Reviewing the experience would be benefit of users of codes such as EMTP.

From the above points of view, this paper introduces first a phase domain modeling, using the first and second order of stable transfer functions [3]. Also a modification of frequency characteristics in very low frequency area to the efficient DC initialization is introduced. The model constructed with these techniques is stable. This model has been installed in EMTP(DCG V2.1). Next, a comparison between field tests and simulated results were made. The comparison involves a DC airline, DC cable and double AC airlines. Lastly comparison between the phase domain model and the constant transformation matrix model were made to the simulation of step and frequency response. This test showed that difference between two models grew with longer simulation time, reaching considerable amount especially in resonance.

2. A MODELING IN PHASE DOMAIN

This modeling bases on observations of phase domain frequency characteristics. Fig.1 shows given attenuation characteristics of 2c.c.t. line. The frequency characteristics of the part of mark A and B in Fig.1 are similar to these of the transfer function (1a) and (1b) respectively. Then the part A and B are approximated with (1a) and (1b). Fig.2 shows the residual which subtracted the frequency characteristics of specified (1a) and (1b) from the given frequency characteristics. The part of mark B and C similar to (1b) and (1c) appear with reduced magnitude level. For further approximation, same situation appears repeatedly. This can be observed in surge admittance of phase domain.

$$f_1(s) = \frac{k}{1+st_d} \tag{1a}$$

$$f_2(s) = k_p\left(\frac{1}{1+st_{d1}} - \frac{1}{1+st_{d2}}\right) \tag{1b}$$

$$f_3(s) = \frac{k_q \varsigma_q \omega_n s}{s^2 + \varsigma_q \omega_n s + \omega_n^2} \tag{1c}$$

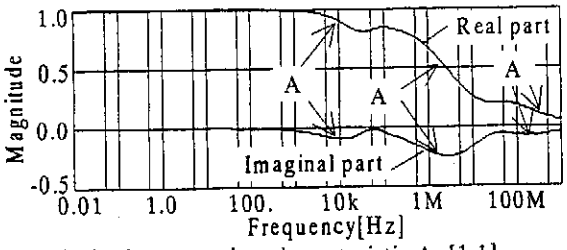

(a)Self-Attenuation characteristic Ap[1,1]

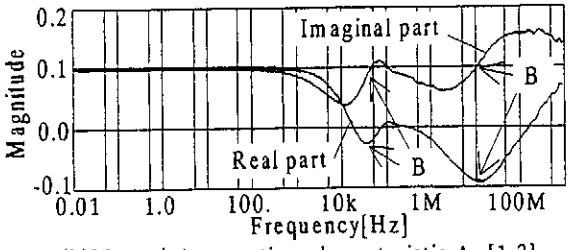

(b)Mutual-Attenuation characteristic Ap[1,2]

Fig.1.Frequency characteristics of attenuation.

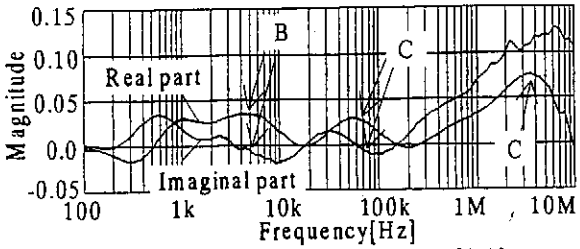

Self-Attenuation characteristic Ap[1,1]

Fig.2. Frequency characteristics of the residual.

From the observation, we developed a successive approximation using the function (1a), (1b) and (1c) as formation function. The algorithm as follows.

Step 1: This step sets the residual subtracted the real value at the highest frequency from the given frequency characteristics. The real value is registered as a fraction of the approximated function set.

Step 2: This step finds a location on the residual to be approximated with a specified function. The location can be identified with scanning of frequency-amplitude pattern and logistic judgment.

Step 3: This step decides coefficients of the specified function. This can be done through normal least square technique using the real part of frequency characteristics of the residual. The coefficients are registered in the approximated function set.

Step 4: This step calculates new residual with the coefficients decided one step before. If the new residual is small enough, then it goes to next step. Else, it goes to Step 2.

Step 5: For surge admittance , the algorithm ends . For attenuation, this step calcurates total frequency characteristics of the registered function set and phase angle. If the deviation of the phase angle to the given one are not small enough,then modify propagation time and the given frequency characteristics, it goes to Step 1. Else the algorithm ends.

The final function set can be described as follows.

$$F(s) = k_c + \sum \frac{k}{1+st_d} + \sum \frac{k_q \varsigma_q \omega_n s}{s^2 + \varsigma_q \omega_n s + \omega_n^2} \qquad (2)$$

In the modeling, the stability problem on formation function is negligible because the approximation process easily accepts stable constraints to those low order functions.Once the approximation of propagation and surge admittance is obtained in the form (2), the time domain recursive convolution is easily obtained [2].

Fig.3 shows the configuration of a DC air line model based on Hokkaido-Honshu DC link. The modeling of attenuation characteristics for 31.2km case of the line are shown in Fig.4. The modification of propagation time as mentioned in the algorithm is illustrated in the enlarged portion in Fig.4. The phase shift of tail part of the given characteristics are adjusted to be able to fit to stable formation function (1a) to (1c). As appears in the figure, the approximated results fit well to the modified characteristics. The number of formation function required for the approximation of the surge admittance and attenuation characteristics are shown in the table 1 and 2.

Now, a modification of the frequency characteristics in low frequency area is illustrated. Suppose that the conductance to the earth can be neglected and frequency is low enough,

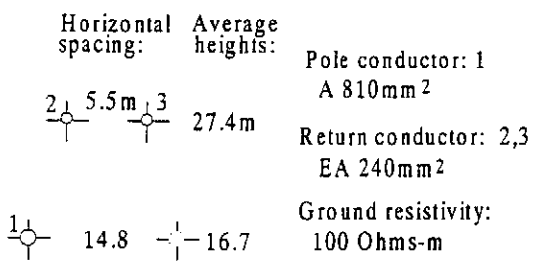

Fig.3. Configuration of a DC air line model.

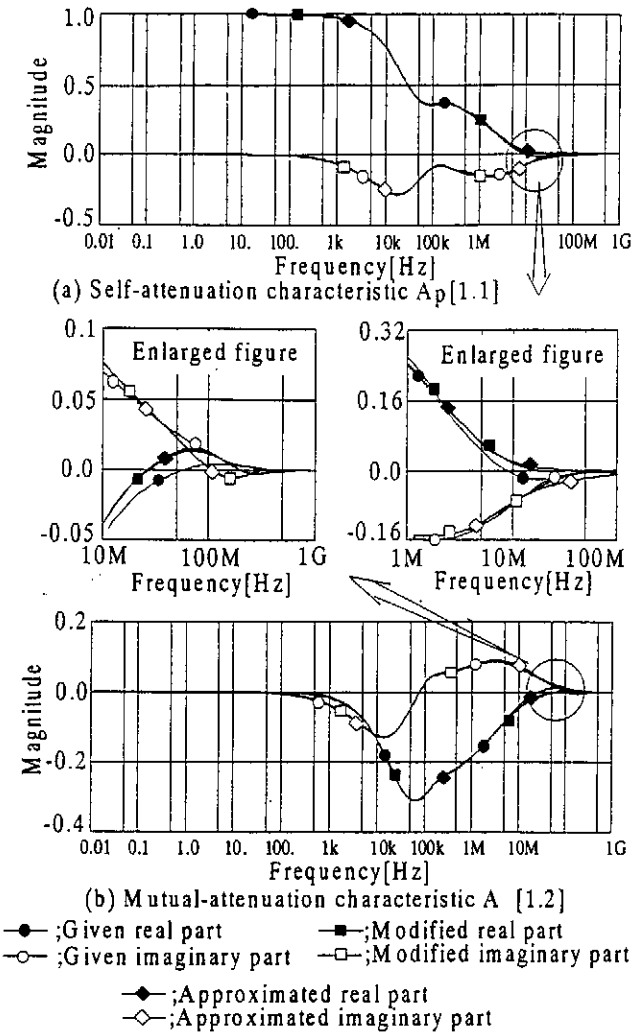

Fig.4. Fitness of the modeling.

Table 1. Results of modeling for surge admittance.

(Frequency range : 0.01Hz to 1000MHz)

Element	Number of $f_1(s)$	Number of $f_3(s)$
(1, 1)	18	11
(1, 2)	19	16
(1, 3)	21	15
(2, 2)	18	1
(2, 3)	14	0
(3, 3)	18	1

Table 2. Results of modeling for attenuation.

(Frequency range : 0.01Hz to 1000MHz)

Element	Number of $f_1(s)$	Number of $f_3(s)$
(1, 1)	7	3
(1, 2)	10	9
(1, 3)	6	17
(2, 1)	12	8
(2, 2)	13	2
(2, 3)	14	11
(3, 1)	8	17
(3, 2)	8	18
(3, 3)	10	9

surge admittance *Ys* and propagation constant *P* may be described as follows.

$$Y_s = (R+sL)^{-1}\sqrt{(G+sC)(R+sL)} \cong \sqrt{CR^{-1}}\cdot\sqrt{s} \quad (3a)$$

$$P = e^{-\gamma l} \cong I - \gamma l = I - \sqrt{CR}\, l\cdot\sqrt{s} \quad (3b)$$

Where $\gamma = \sqrt{(G+sC)(R+sL)} \cong \sqrt{CR}\cdot\sqrt{s}$, and *R, C, l* and *s* are resistance and capacitance matrix, line length and Laplace operator respectively.

Here, in (3a) and (3b), let's replace square root of *s* to small positive constant α, then the impedance *Ze* and admittance *Ye* of pi-equivalent can be derived as follows.

$$Z_e = Y_s^{-1}\sinh(\gamma l) \cong Rl \quad (4a)$$

$$\frac{Y_e}{2} = Y_s\frac{\cosh(\gamma l)-I}{\sinh(\gamma l)} \cong \frac{\alpha^2 Cl}{2} \quad (4b)$$

In (4b), even the capacitance changes it's nature to the conductance, with small α, the influence to affect DC initialization may be neglected, and still capacitive voltage distribution may be maintained. Fig.5 illustrates the modification of surge admittance case. The square root of s characteristics is discarded, being replaced to real constant. This modification makes the approximation in low frequency area easier, reducing number of term of formation function.

A 650kV class of 2c.c.t. DC line model, of which distance is 370km, was tested with the constant 1 as α. The receiving-end voltage was set to 650kV, the sending-end voltage to 650kV plus voltage drop of DC current 2500A. The DC current error of the code output was -0.02% at the receiving-end. Fig.6 shows voltage response when a power line is energized with step voltage source. For the 1sec run, the response is stable, reaching and remaining the capacitive voltage distribution.

3. FIELD AND PHASE MODEL TESTS

In the following tests, Field test records by oscilloscope are digitized to agree with the simulated voltage at the time near by crest, since the record of voltage scale has been lost. Then only the waveform can be examined.

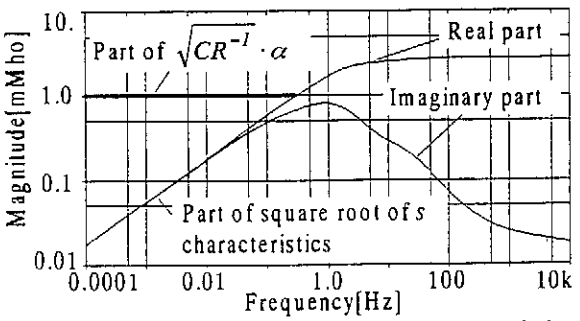

Fig.5. Modification of square root of *s* characteristics.

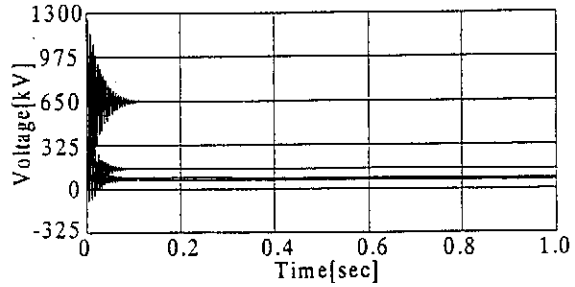

Fig.6. Step voltage response.

3.1 A 250kV class DC overhead line

This line consists of 1 power wire and 2 return wires in the stage tested as shown in Fig.3. The test line distance was 31.2km. An impulse wave, 45/4000 μsec, was applied to the power wire. Fig.7 compares field test results with simulated results. In the figure, The mark F and S denotes field test and simulated result respectively. Though the waveform agrees well each other, still the difference remains at the detail. The difference arises at each buildup and trailing section of wave. These difference may be affected with data such as impulse generator, average heights, ground conductivity. For better simulation, the examination on those data are required.

3.2 A 250kV class DC submarine OF cable

The test line distance was 44.4km. The cable sheath and armoring are bonded every 3.6km. An impulse wave, 1/36 μsec, was applied to the power conductor. Each segment of the cable is modeled with 2 conductors system consisting of the power conductor and the sheath. Fig.8 shows the voltage responce of the power conductor. The ratio of the first peak to the second of field test result agrees well with that of the simulated result. The difference exists in the trailing section of the wave. This may be affected with the impulse generator constants.

3.3 A 500kV class AC vertical overhead line

The line configuration is shown in Fig.9. The test line distance was 42km. An impulse wave, 1/4000μsec, was applied to the bottom phase. The waveform of the simulated

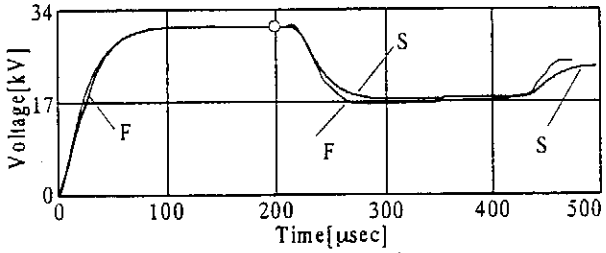

(a) Voltages on conductor 1

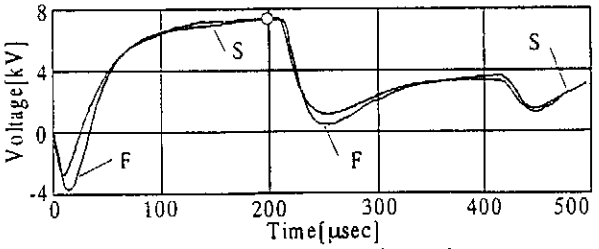

(b) Voltages on conductor 2

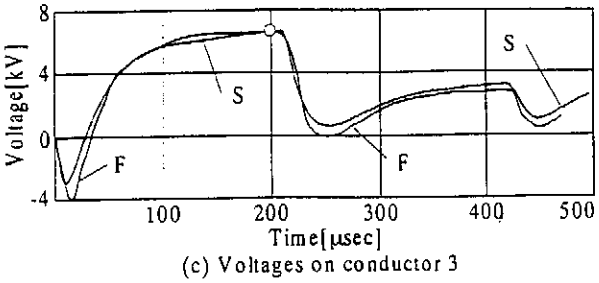

(c) Voltages on conductor 3

Fig.7. Impulse response of a 250kV DC overhead line.

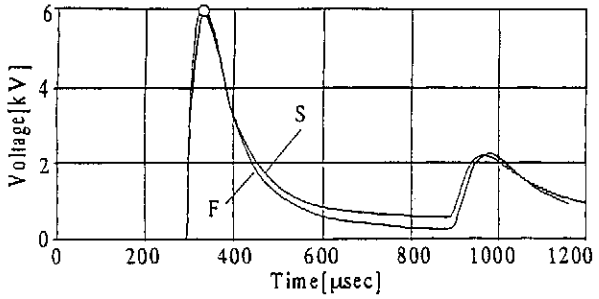

Fig.8. Impulse response of a DC submarine cable line.

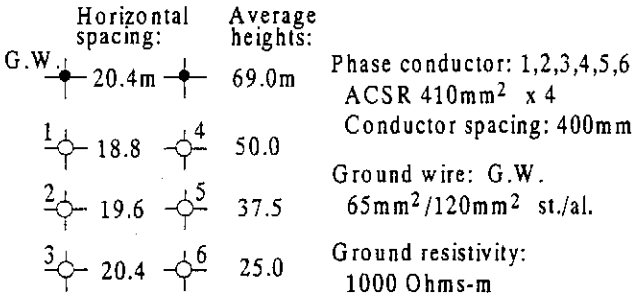

Fig.9. Configuration of a AC vertical overhead line.

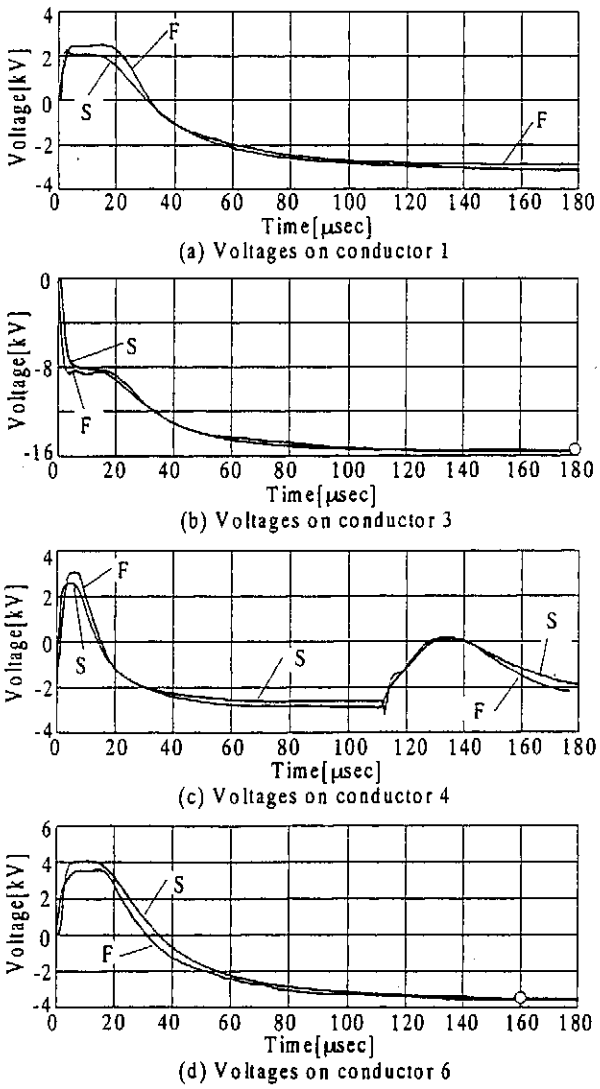

Fig.10. Impulse response of a vertical overhead line.

results agrees well to those of the field test results as shown in Fig.10.

4. COMPARISON BETWEEN MODELS

A comparison work between the phase domain model(PD) described before and a constant transformation matrix model(CTM) has been done. The CTM of EMTP (DCG v1.2) was selected as a standard one. Step energizing and frequency response tests were done to examine the behavior for longer simulation time.

4.1 Model lines

Three model lines were tested. Fig.11 shows the configuration of a triangular overhead AC line. The line distance is 222km. Fig.9 shows a vertical overhead AC line mentioned before. The distance is 200km. Fig.12 shows the configuration of a two bipole overhead DC line which has two return wires. The line distance is 375km.

4.2 Step energizing test

In the following, the test case which produces the larger difference between CTM and PD in each test is presented.

4.2.1 A triangular overhead AC line

Fig.13 shows the voltage waveform on the receiving-end terminals, when the bottom phase of the sending-end was energized by the unit step voltage and other terminals remain open. Difference between CTM derived at 1kHz and PD to the positive peak voltage in the first wave is 2% on the energized phase and 3.9% on the top phase, i.e., the induced phase. While the difference of the third wave's peak voltage is 4% on the energized phase. For CTM simulation, the transformation matrix were derived at different frequency. The choice of the frequency did not make great change in this case as shown in Fig.13.

Fig.14 shows the case that the top phase was energized. Difference between CTM at 1kHz and PD to the positive

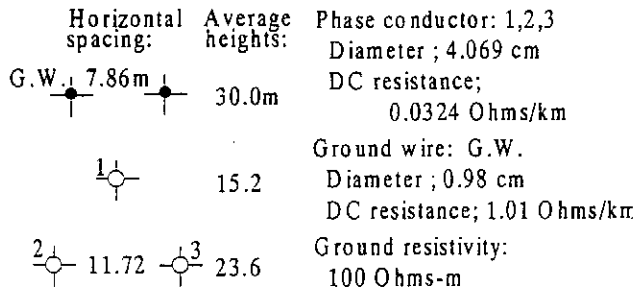

Fig.11. Configuration of a triangular overhead AC line.

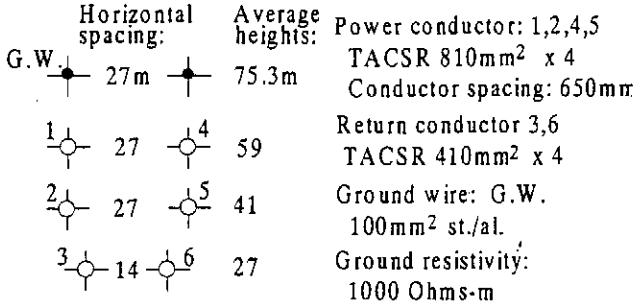

Fig.12. Configuration of a two bipole overhead DC line.

peak voltage in the first wave is 3% on the energized phase and 1.1% on the induced phase. While the difference of the third wave's peak voltage is 10.4% on the energized phase, 9% on the induced phase. CTM at 300Hz reduced the difference of the third wave's peak voltage on the energized phase to 8%.

4.2.2 A vertical overhead AC line

Fig.15 shows the voltage waveform on the bottom phase of the receiving-end , when the same phase of sending-end was energized. Difference between CTM at 1kHz and PD of the positive peak voltage in the first wave is 1.4%, then growing 3.4% in the third wave. The waveform of first wave resembles well at the detail each other as shown in the enlarged figure of Fig.15. The maximum difference of the first wave in induced phase was 4.7% in the top phase.

4.2.3 A two bipole overhead DC line with return wires

Fig.16 shows the voltage waveform on the top of power conductor, when the same conductor of sending-end was energized. The difference of the positive peak voltage in the first wave is 2.1%, then growing 3.6% in the third wave. The maximum difference of the first wave in induced conductors was 8.5% in the return wire, when the middle power conductor was energized.

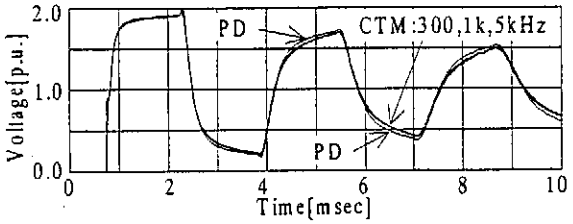

(a) Voltages on conductor 1

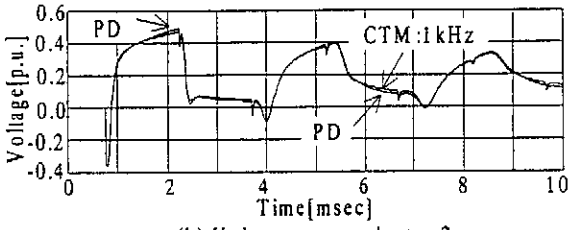

(b) Voltages on conductor 2

Fig.13. Step response of a triangular overhead AC line. (The bottom phase energizing case)

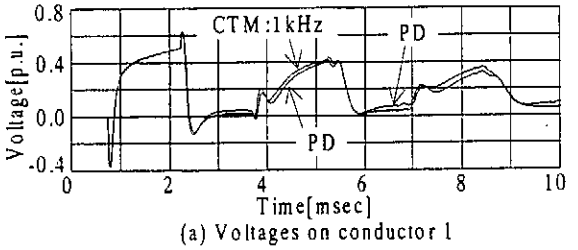

(a) Voltages on conductor 1

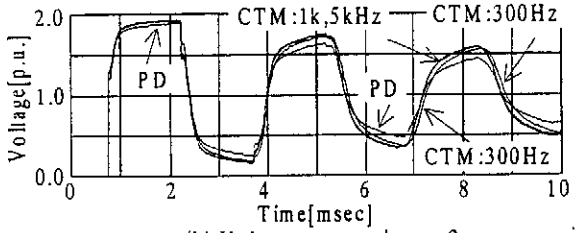

(b) Voltages on conductor 2

Fig.14. Step response of a triangular overhead AC line. (The top phase energizing case)

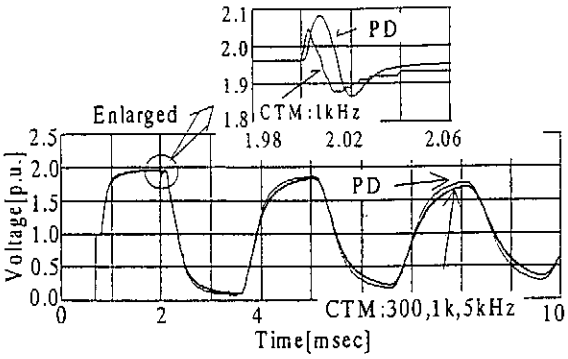

Fig.15. Step response of a vertical overhead AC line.

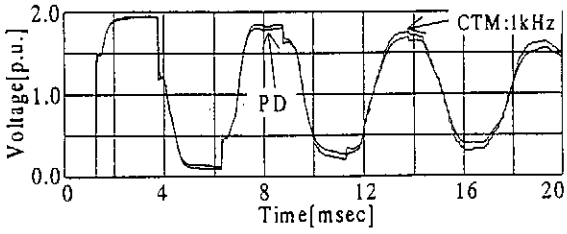

Fig.16. Step response of a two bipole overhead DC line.

4.3 Frequency response test

The Frequency responses of the CTM and PD can be obtained as the value when the simulation using those reaches steady state. Also, the exact frequency solution is obtained with nodal equation. The error of the models can be evaluated with the exact frequency solution. In the following, the test case which produces the larger error for CTM in each model line is presented.

4.3.1 A triangular overhead AC line

Fig.17 shows the error of CTM derived at 1kHz and PD, when the sinusoidal voltage was applied to the top phase. The maximum error of PD is less than 1%. While the maximum error of CTM is about 40% at 310Hz, the first resonance frequency of the circuit, on the top phase.

4.3.2 A vertical overhead AC line

Fig.18 shows error of the models when the sinusoidal voltage wave was applied to the bottom phase. The error of PD remain within 1% for all frequency. While the error of CTM reaches about 20% at 317Hz.

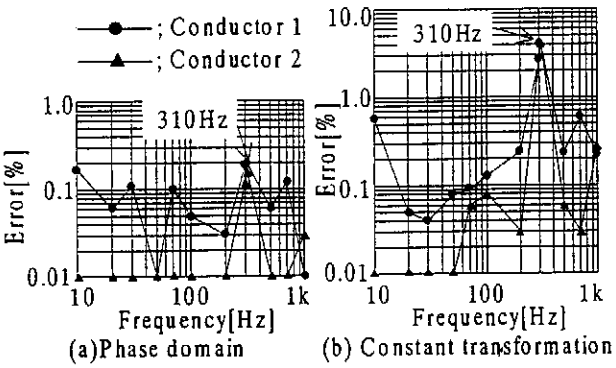

(a)Phase domain (b) Constant transformation

Fig.17. Frequency response of a triangular. overhead AC line

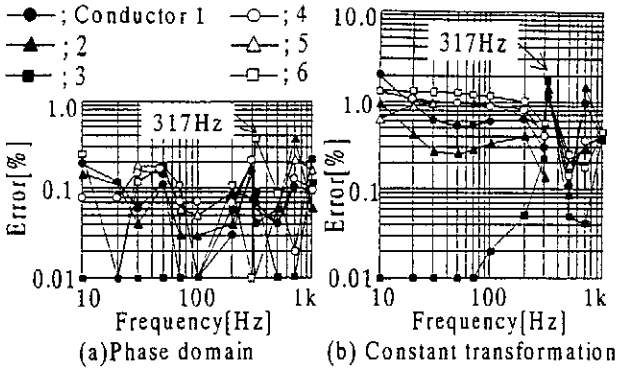

Fig.18. Frequency response of a vertical overhead AC line

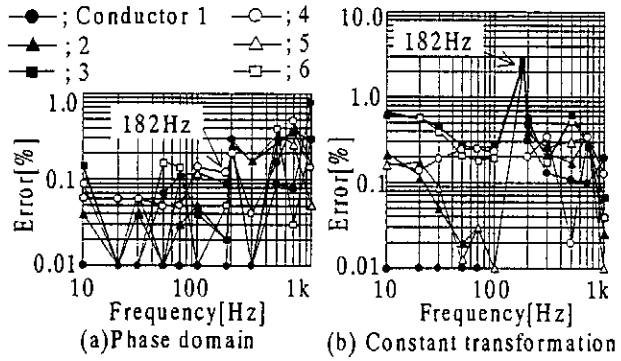

Fig.19. Frequency response of a two bipole DC line with two return wires

4.3.3 A two bipole overhead DC line with return wires

Fig.19 shows error of the models when the sinusoidal voltage wave was applied to the middle conductor and other terminal remain open. The error of PD are within 1% for all frequency. While the error of CTM reaches 24% at 317Hz on the receiving end of the energized conductor.

5. CONCLUSION

A phase domain model was introduced and it's outputs were compared with field tests, theoretical frequency solutions and the outputs of a constant transformation matrix model. From those works, the following can be concluded.

(1) The modeling introduced in this paper can offer the accurate and stable phase domain model.

(2) Though the phase domain model produces waveforms which agree well with field test results, still disagreement remains at the detail. This disagreement may be affected with data such as impulse generator, average heights, ground conductivity. The careful examination of those data is still very important for better simulation.

(3) The difference between the phase model and a constant transformation matrix model is comparably small in short time transient such as the first wave analysis. The maximum difference of the first wave was 3% in energized conductor, 8.5% in induced conductor. While the difference of two models grew with longer simulation time, reaching considerable amount especially in resonance.

Phase domain model is the more important in the larger time span of simulation.

6. REFERENCES

[1] T.Ino, C.Uenosono,"An examination of highly accurate equivalent circuit for double-circuit DC transmission line.",T. IEE Japan, vol.114B, No. 5, May 1994.

[2] A. Semlyen, A. Dabuleanu, "Fast and accurate switching transient calculations on transmission lines with ground return using recursive convolution ", IEEE Trans., Vol.PAS-94,No.2, March/April, 1975.

[3] T. Ino, C. Uenosono,"An approximation method of frequency dependent effect in phase frame for unbalanced transmission line.", T. IEE Japan, vol.113B, No. 12, December 1993.

[4] G.Angelidis, A.Semlyen,"Direct phase domain calculation of transmission line transients using two-sided recursions", IEEE Trans. on Power Delivery, Vol.10, No.2, April 1995

[5] T.Noda, N.Nagaoka, A.Ametani,"Phase domain modeling of frequency dependent transmission lines by means of ARMA model.", IEEE Winter Meeting, 95 WM 245-1PWRD,January 11, 1995.

[6] T. Ino, C. Uenosono,"An examination of a phase frame modelling for transients of unbalanced transmission lines with Bergeron method.", T.IEE Japan, Vol.115B, No.9, September, 1995.

[7] B. Gustavsen, A. Semlyen,"Simulation of transmission line transients using vector fitting and modal decomposition.", IEEE Trans. on Power Delivery, Vol.13, No.2, April 1998.

[8] B. Gustavsen, A. Semlyen," Calculation of transmission line transients using polar decomposition.",IEEE Trans. on Power Delivery, Vol.13, No.3, July 1998.